

© 2020 IEEE. Personal use of this material is permitted. Permission from IEEE must be obtained for all other uses, in any current or future media, including reprinting/republishing this material for advertising or promotional purposes, creating new collective works, for resale or redistribution to servers or lists, or reuse of any copyrighted component of this work in other works.

Alternative Radiated Susceptibility Test Methods at Unit Level

Sergio A. Pignari, Giordano Spadacini, Flavia Grassi

Department of Electronics, Information and Bioengineering, Politecnico di Milano

Email: sergio.pignari(giordano.spadacini, flavia.grassi)@polimi.it

Abstract—This article briefly illustrates and discusses the possibility to develop alternative, simplified test methods for radiated susceptibility testing at unit level, for the aerospace sector. The rationale here discussed, and the alternative test methods here illustrated are targeted to the development of a more physically sound, quicker, and less expensive testing approach in order to help the industrial design process of equipment for spacecraft. The theoretical basis of this analysis is the possibility to enforce equivalence (in terms of common mode current) among the effects due to field-to-wire-coupling, bulk current injection and crosstalk, under suitable assumptions. Two dual approaches are considered, one aimed at achieving deterministic equivalence, the other enforcing equivalence in statistical terms. Pros and cons of the proposed alternative test methods are discussed by illustrating the outcomes of ad hoc setups and a wide experimental campaign.

Index Terms—Aerospace EMC, EMC testing, radiated susceptibility (RS), conducted susceptibility (CS), Bulk current injection (BCI).

I. Introduction

Compliance of spacecraft with radiated emission (RE) and susceptibility (RS) limits is of crucial importance in aerospace. Indeed, in spacecraft for earth observation, navigation and telecommunications, very sensitive sensors, on-board receivers and diversified types of payloads are usually required to operate in densely populated environments, in close proximity with strong RF transmitters, high power DC/DC converters and high-speed data links. Accordingly, in order to guarantee electromagnetic compatibility (EMC) at spacecraft level, each electronic unit mounted on-board shall undergo complex, severe, expensive, and time consuming RE and RS tests. Concerning susceptibility, tests are obviously targeted to avert performance degradation or damage during spacecraft operation. Currently, both RS and conducted susceptibility (CS) test procedures are foreseen to assess equipment immunity by the international standards of the aerospace sector [1]-[3], and different tests coexist at low frequencies. Even though those tests are aimed at investigating different phenomena and their co-existence may be consistently foreseen, the presence of multiple tests and overlapping frequency ranges, the test complexity and execution costs point out the need for correlation of the tests outcomes and the possibility for identifying alternative, simplified test methods. Further, if a rationale can be developed for correlating RS and CS tests, the testing methodologies and

associated frequency ranges could be rationalized, possibly considering CS tests (involving inherently simpler setups) as a complement, or even substitute of RS verifications at unit level.

In line with the aforementioned context, this work briefly reviews and comments on some alternative methods for RS testing that were recently investigated and proposed. It will be shown how these tests could improve repeatability (sometimes difficult at low frequencies), and lead to time and cost savings when testing is considered from an industrial point of view. The main theoretical feature of the tests methods here illustrated is that they assure equivalence between CS and RS in terms of common mode (CM) RF currents injected in the units under analysis. Equivalence of the resulting differential modes (DMs) is therefore obtained as a by-product. Two merely different test approaches will be considered, one aimed at achieving deterministic equivalence, the other targeted to statistical equivalence. These approaches are complementary both in the theoretical rationale as well as in the practical implementation. In all the examples addressed in this article, the electromagnetic field generated by the antenna (see Fig. 1) will be approximated by a uniform plane wave.

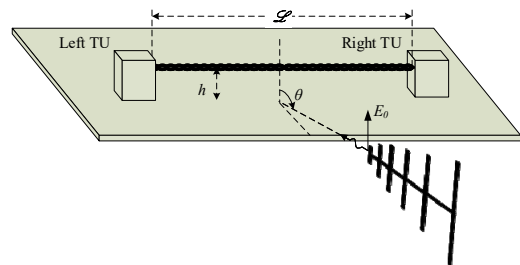


Fig. 1—Principle drawing of a test setup for RS testing at unit level, according to EMC standards [1]-[3].

II. Alternative tests enforcing exact equivalence with RS

This section introduces the basic principles of alternative test methods assuring exact equivalence with RS.

The proposed methods are based on:

- (a) Conducted-noise injection by the use of two identical injection devices clamped at the ends of the harness under test. Devices suitable to this purpose are injection probes currently foreseen by the international standards for CS verifications. Particularly, since the implementation presented in this work involves two bulk current injection (BCI) probes, the proposed method is hereinafter denoted as double BCI (DBC) procedure.

(b) Noise induction through near-field coupling, by crosstalk with a generator circuit placed in close proximity to the bundle under test, suitably fed at both terminations.

The proposed schemes of equivalence offer the advantage of implementing rigorous deterministic equivalence with RS for whatever incidence direction and polarization of the impinging wave and, in particular, for both the vertical and horizontal polarizations, and the antenna positioning (see Fig. 1) foreseen in the standards of the aerospace sector [1]-[3].



Fig. 2 – Equivalent representation of a system undergoing the RS test: The two equivalent voltage sources connected at the ends of the harness represent the electromagnetic CM noise induced by the impinging field.

The rationale for these test methods stems from the equivalent representation (see Fig. 2) of the harness under test in the RS setup, where the RF energy picked up from the electromagnetic field generated by the antenna (see Fig. 1) is modeled by two equivalent RF voltage sources lumped at the bundle ends [4]. Since here the objective is to exactly reproduce by CS the CM noise currents/voltages induced in both the terminal units (i.e., two target variables), the use of two independent RF generators controlled both in magnitude and phase shift is required.

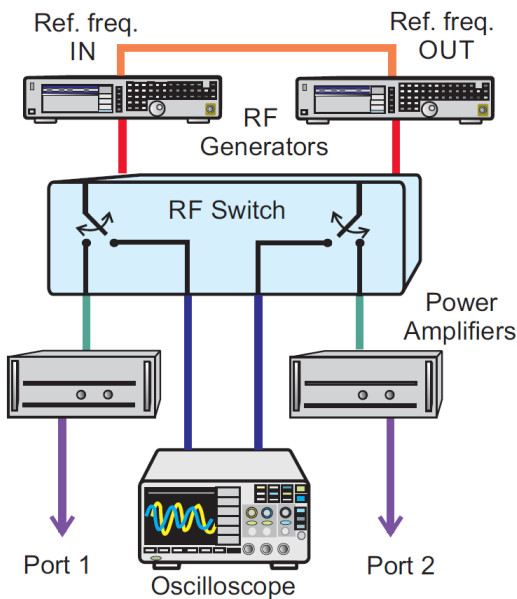


Fig. 3 – Block diagram of the alternative test setup based on DBCI and crosstalk.

Particularly, the relative phase shift needs to be controlled since any current and voltage in the circuit will result from the superposition of the effects of both the sinusoidal sources.

a) Test setup and procedure

A principle drawing of the proposed setup is shown in Fig. 3, where port 1 and 2 are connected either to two identical BCI probes (DBCI procedure) or to the terminations of the generator wire (crosstalk-based procedure). All coaxial cables drawn with equal colors have the same length. The two RF sources share the same 10 MHz reference-frequency oscillator in order to exactly generate the same frequency. To this aim, the “Ref. In” and “Ref. Out” ports available on the rear panel are connected. Test execution is controlled by *ad hoc* LabView routine running on a computer interfaced with all instruments through USB and GPIB ports.

For each frequency point, a preliminary calibration is carried out. Calibration is aimed at setting the desired phase shift between the two generators. Every time a new frequency and the corresponding forward power are set, the two generators are switched on. The random phase shift observed between the generated sinusoids is then measured through an oscilloscope, and acquired by the computer, which enforces the desired phase shift by correcting the phase of one of the two generators. After calibration, the switch connects the generated signals to ports 1 and 2 and the test is executed.

In order to validate the proposed schemes of equivalence, a spectrum analyzer, properly controlled by the same computer, is included in the setup to monitor the CM current injected in one of the terminal units during the test, and to compare it versus the theoretical value resulting from the RS test.

b) DBCI test

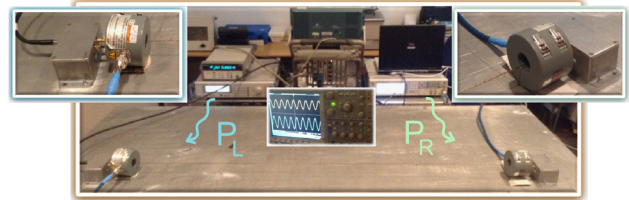


Fig. 4 –DBCI setup: Two identical probes are clamped next to the terminal units, and oriented in opposite directions.

A picture of the DBCI test setup is shown in Fig. 4. The harness under test is a 1.5 m long twisted-wire pair (TWP) with possibly imbalanced terminal loads (enclosed into metallic boxes), at the height $h = 20$ mm above a metallic plane. Two injection probes FCC F-130A are clamped at the ends of the TWP and oriented in opposite directions.

By imposing equal magnitude of the CM currents I_L , I_R (see Fig. 2) induced by RS and by DBCI, respectively, the forward power and the phase shift required for the two RF sources can be analytically determined. However, this operation does not lead to a unique answer. Among the possible solutions, the DBCI implementation here proposed involves the magnitude and phase shift of the two RF generators which minimize the RF forward power required to run the test, [5]. Such analytical expressions (not explicitly reported for brevity) can be written

in simplified form as:

$$P_{L(R)}(f) = f_1(I_L, I_R, \Gamma_{LP}, \Gamma_{RP}, H_P, L / \lambda_0), \quad (1)$$

$$\Delta\phi(f) = f_2(I_L, I_R, \Gamma_{LP}, \Gamma_{RP}, L / \lambda_0), \quad (2)$$

where H_P denotes the frequency-dependent probe coupling factor, and Γ_{LP} and Γ_{RP} are the actual reflection coefficients at the left (L) and right (R) ends. Namely, Γ_{LP} and Γ_{RP} account for the difference between the CM characteristic impedance of the harness and the equivalent CM impedance of the load, that is the series connection between the probe series impedance (i.e., impedance Z_P in [6]), and the load impedances $Z_{CM,L}$ and $Z_{CM,R}$, respectively. Moreover, λ_0 denotes the wavelength at frequency f in free-space. As a matter of fact, since equivalence is enforced in terms of CM only, the presence of dielectric material surrounding the wires in the TWP can be neglected as long as evaluation of the forward power is the target.

It is worth noting the dependence of (1) and (2) on the two load currents induced by RS. This entails the need to know the CM impedance of the terminal units (information not always available to the operator). On the other hand, such a dependence provides a way to extend the proposed DBCI to the more general case of non-uniform electromagnetic fields illuminating the harness, on condition that I_L, I_R are known [5]. The validation proposed here refers to the conditions of incidence imposed by typical RS setups foreseen by the international standards in [1]-[3], where the antenna is placed in front of the harness under test, at midpoint (broadside incidence, $\psi = 180^\circ$), at a distance d_a and height h_a , so that $\theta \approx \arctan(d_a/h_a) \approx 73^\circ$. The test is repeated with the antenna in vertical (VP, $\eta = 0^\circ$) and horizontal polarization ($\eta = 90^\circ$). For VP, the forward power required to feed the two BCI probes and the corresponding phase shift between the two RF sources are plotted in Fig. 5, for unitary electric-field strength $E_0 = 1$ V/m. Accuracy of the proposed procedure in reproducing the CM current induced by RS in one of the terminal units is assessed in Fig. 6, where the solid curve was obtained by prediction, whereas crosses denote the measurement points obtained by running the DBCI test.

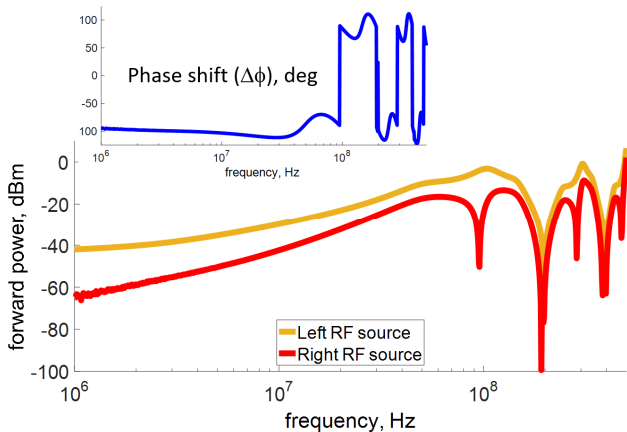


Fig. 5 – Example of feeding conditions: Broadside incidence with the antenna in vertical polarization.

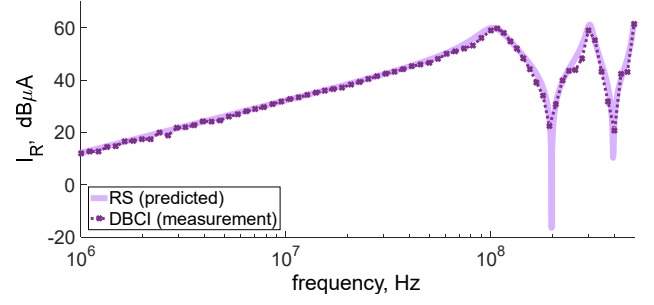


Fig. 6 – CM current entering the right terminal unit: Radiation (prediction) vs DBCI (measurement).



Fig. 7 – Setup used for validation of the crosstalk based procedure.

c) Crosstalk-Based test

A picture of the alternative test setup based on crosstalk is shown in Fig. 7. The harness under test is the same TWP involved in the DBCI setup in Fig. 4. However here, instead of the BCI probes, a generator wire fed at both ends as described in Subsection II.a, parallels the TWP at distance $\Delta = 30$ mm.

With reference to the equivalent representation of the RS setup in Fig. 2, suitable feeding conditions for the RF sources feeding the generator wire can be obtained by enforcing equivalence in terms of equal voltage sources induced by RS and crosstalk at the ends of the harness [7]. Here, a fundamental assumption is that the presence of the generator wire does influence the passive part of the model of the harness under test (when subject to crosstalk). This condition is satisfied as long as (a) the two wiring structures are weakly coupled [8], and (b) the generator wire is matched (in the setup in Fig. 7, matching was achieved by soldering 250Ω resistors in series with the end-points of the generator wire), [7].

As a consequence, here the feeding conditions of the two RF sources are univocally determined, do not depend any longer on the impedance of the terminal units, and can be expressed as functions of the following parameters:

$$P_{L(R)}(f) = f_3(\hat{V}_{SL}, \hat{V}_{SR}, L / \lambda_0, k), \quad (3)$$

$$\Delta\phi(f) = f_4(\hat{V}_{SL}, \hat{V}_{SR}, L / \lambda_0), \quad (4)$$

where k is the coupling coefficient between the generator wire and the equivalent wire of the CM model of the harness under

test, whereas V_{SL} , V_{SR} denote the equivalent voltage sources induced by RS. The effect of dielectric coating is neglected in the derivation of (3)-(4), since the target is reproducing the induced CM current only [9].

To reproduce the incidence conditions foreseen by the standards [1]-[3], theory shows that the setup in Fig. 7 has to be fed by two RF sources with equal magnitude and phase shift constant over frequency (i.e., $\Delta\phi = 0^\circ, 180^\circ$ for VP and HP, respectively). The required forward power for VP and HP, respectively, is plotted in Fig. 8(a). As a general result for typical antenna positioning (leading to elevation angle $\theta \approx 73^\circ$) foreseen by the standards, only VP is required, as it involves more severe test conditions than HP. As an example of results, Fig. 8(b) shows the comparison between the theoretical predictions of the CM voltage induced by RS (VP) and the actual CM voltage measured in the alternative setup based on crosstalk. To prove validity of the feeding conditions shown in Fig. 8(a) in spite of the specific loads, the test was repeated for two different CM impedances of the terminal units (i.e., 25Ω and $1 \text{ k}\Omega$).

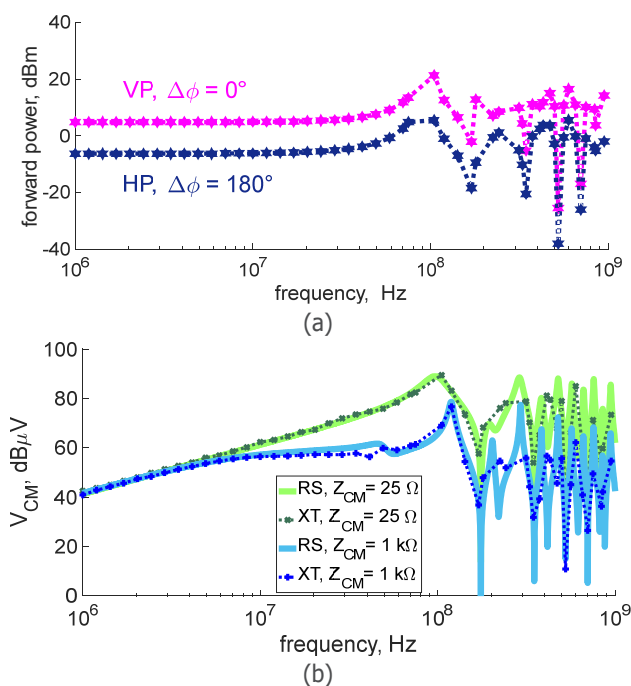


Fig. 8 – (a) Forward power for VP and HP; (b) CM voltage at one termination of the harness for two different CM impedances of the terminal units.

III. Alternative test enforcing equivalence in statistical terms

As discussed in the previous section, deterministic approaches to the equivalence between RS and CS involve complex test setups (e.g., two independent RF sources, computer-controlled instruments, etc.) and knowledge of parameters (e.g., the CM impedance of the units under test) which are often unknown/uncontrolled to the test operators. This complexity is often incompatible with typical industrial requisites, such as the need for fast pre-compliance verifications. Accordingly, the test method described in the following is aimed at establishing a

test procedure whose outcome is not exactly equal to the expected outcome of an RS test, though statistically correlated with it. Such a relaxation of the final objective is the key to achieving reproduction of the RS effects while retaining the practicality of common test procedures.

The following basic concepts are used:

1. The proposed test method is based on BCI and conforms to the conventional calibration method foreseen by many standards. Reference test levels are defined as suitable frequency profiles of the RF current to be injected in the 50Ω terminal load of a “substituted” test setup with controlled characteristics, namely, the standard BCI calibration fixture [1], [10]. The forward power needed to feed the BCI probe in the calibration setup is recorded, frequency by frequency, and subsequently used to feed the BCI probe in the actual test setup.
2. The proposed test levels are piecewise-linear frequency profiles properly designed to achieve correlation with the corresponding RS test. Therefore, they are associated with some reference RS test conditions (e.g., electric field amplitude), setup geometry (e.g., height of the cable above ground), separately specified for VP and HP, and unshielded/shielded cables under test.
3. Simple scaling rules allow tailoring the proposed test levels to setup parameters different from the reference values.
4. The proposed test levels can be associated with statistical information on the BCI test severity, given in terms of probability that the injected disturbance exceeds the disturbance that would be induced by the RS test.

a) Relationship among BCI and RS test levels

The parameters of interest in the RS test setup are illustrated in Fig. 1, and the following values are assumed as reference conditions: Electric field strength (unperturbed incident field) $E_0 = 1 \text{ V/m}$; antenna elevation angle (from the vertical direction) $\vartheta = 73^\circ$; cable height above ground $h = 0.05 \text{ m}$; cable length $\mathcal{L} = 2 \text{ m}$.

The system is composed of two terminal units interconnected by an unshielded/shielded cable harness, running above a metallic ground plane. Both terminal units are functionally considered as the equipment under test. The antenna can be operated in VP or HP.

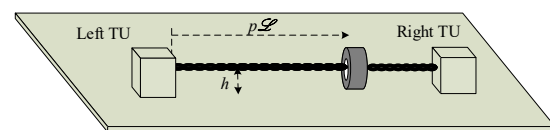


Fig. 9 –BCI test setup.

As shown in Fig. 9, the BCI test is performed in a similar setup, retaining the same cable length and height. The coupling device is a BCI probe clamped on the cable harness at a certain relative distance from the left unit (described by the dimensionless parameter p , $0 \leq p \leq 1$).

The proposed reference test levels (RTLs) are plotted in Fig. 10 for the abovementioned reference conditions of the RS test

[10], [12]. It is worth noting that all test levels involve a sloped segment at low frequencies, where the cable is electrically short [hereinafter we will use the acronym ESL (electrically short line) to identify this frequency range], and a high frequency horizontal segment, where the cable is electrically long [ELL (electrically long line) is the acronym used for this frequency range]. In Fig. 10, f_s is the separation frequency between the two aforementioned frequency ranges. The slope of the ESL segment is +20 dB/decade and $f_s = 24$ MHz for all cases except case SH-VP which has +60 dB/decade slope and $f_s = 36$ MHz. To account for different testing conditions, the simple rules in Tab. 1 are to be used for rescaling the test levels and f_s . Given the typical frequency range and cable length involved in RS test procedures, the ELL range of the test levels is often of major interest with respect to the ESL range.

The maximum frequency in Fig. 10 was set to 1 GHz, as this frequency represents the ultimate goal for the proposed analysis. This in consideration of the following arguments: (a) the frequency limit of BCI probes; (b) the increasing importance of direct field coupling to the circuits in the terminal units at frequencies in the GHz range, which cannot be mimicked by merely injecting CM currents in the interconnecting cable.

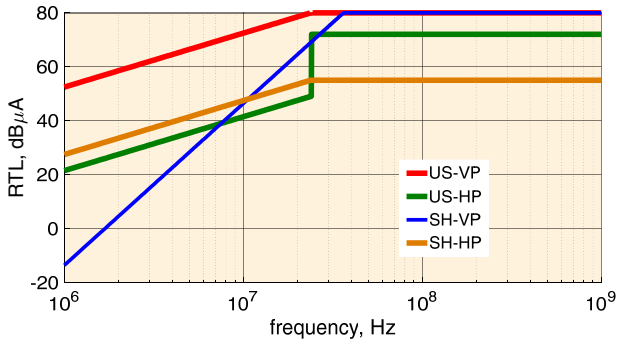


Fig. 10 – Proposed test levels for probe calibration in the standard 50 Ω calibration fixture (US=unshielded cables, SH=shielded cables). The reference test conditions are: $E_0 = 1$ V/m, $\vartheta = 73^\circ$; $h = 0.05$ m; $\mathcal{L} = 2$ m (for other conditions refer to Tab. 1).

TABLE I

RULE TO RESCALE RTLs: $RTL + n \log_{10}(y)$
 RULE TO RESCALE f_s : $f_s \times 2 / \mathcal{L}$

	For VP	For HP
Field Strength	$n = 20; y = E_0/1$	$n = 20; y = E_0/1$
Elevation Angle	$n = 20; y = \sin \vartheta / \sin 73^\circ$	$n = 20; y = \cos \vartheta / \cos 73^\circ$
Line Height	$n = 20; y = h/0.05$	$n = 20; y = h/0.05$
Line Length (ESL)	Unshielded: $n = 20$; Shielded: $n = 60$;	$n = 20; y = \mathcal{L}/2$
" " (ELL)	$y = \mathcal{L}/2$ $n = 0$ (no changes)	$n = 0$ (no changes)

b) The concept of random overtesting

The test levels (RTLs) illustrated in Fig. 10 have been determined to inject by BCI, in most of the cases, a larger disturbance with respect to radiation (RS). Correlation with stress levels induced by radiation can be expressed by the quantity

$$OT = 20 \log_{10} \left| \frac{I_{TU}^{(BCI)}}{I_{TU}^{(RS)}} \right|, \quad (5)$$

hereinafter referred to as "overtesting", where $I_{TU}^{(BCI)}$ and $I_{TU}^{(RS)}$ are the CM currents in the input ports of the terminal units, generated by BCI and RS, respectively. As shown in [10], [12], OT depends on some critical setup parameters of uncertain or unknown value. In particular, it is markedly affected by a) the CM impedance of the terminal units; b) the dielectric permittivity of the insulation material, which has high impact on the CM propagation speed for shielded cables; c) the probe positioning along the cable. Moreover, OT is differently affected by these parameters at different frequencies.

Obviously, OT assumes specific and deterministic values for any specific test setup and frequency. However, from the standpoint of the test operator, OT shall be considered as a random variable. Indeed, the operator lacks knowledge about the abovementioned parameters. Moreover, the test operator usually has to deal with several different setups during his activity, all subject to immunity verifications under the same test procedure.

The severity of a BCI test level can be quantified in statistical terms by considering the cumulative distribution function (cdf) of the random variable OT, that is the probability

$$F(x) = \Pr\{OT \leq x\}. \quad (6)$$

The basic idea underlying the proposed test method is that the OT cumulative distribution function can be predicted by a simulation model based on reasonable statistical assumptions. To this aim, in [10], [12] the RS and BCI test setups in Fig. 1 and Fig. 9, respectively, were simulated by simplified distributed-parameter circuit models retaining just the dominant effects (e.g., coupling and propagation of CM interference in the cable under test). The CM impedance of aerospace equipment and the CM propagation speed were assigned uniform distributions in appropriate ranges inferred from experience in the field and real measurements. Equally, the normalized probe position p was treated as a uniformly distributed random variable. In this connection, it was observed that random probe positioning implies different standing waves of voltage and current along the cable, which has the beneficial effect of augmenting the set of possible outcomes of the test (i.e., widening the variation range of OT with larger and smaller values). Hence, there is no reason to set probe position in the framework of a statistical approach to BCI testing.

This analysis can be performed once and for all with reference to a specific BCI probe (whose accurate circuit model is to be included in the setup model). For the proposed test levels in Fig. 10, and for a BCI probe of type FCC F-130A (maximum frequency 500 MHz), OT cumulative distribution functions are shown in Fig. 11 for the ELL frequency range. The quantiles (or percentiles) of the cdf provide quantitative information on test severity. For instance, the 0.95-quantile corresponds to a value of x around 42 dB in all the four cdfs, which means 95% probability that $OT \leq 42$ dB. The median value of OT (0.5-quantile)

ranges from 18 dB (shielded-VP) to 24 dB (unshielded-HP). One can readily note that use of the proposed test levels leads to $OT \geq 0$ in the vast majority of the cases. Indeed, the probability of undertesting (i.e., $OT \leq 0$) is negligible for unshielded cables and less than 3% for shielded cables. One can demonstrate that the cdfs do not change when the test levels are scaled by the rules in Tab. 1 [10]. Further, it is worth noting that relaxing or increasing the test severity can be readily implemented by simply shifting (up or down) the test levels by Δ dB (where Δ determines the amount of increase or reduction of the test severity). Indeed, this operation simply shifts (to the left or right) the quantiles by Δ dB along the x axis in Fig. 11 [10].

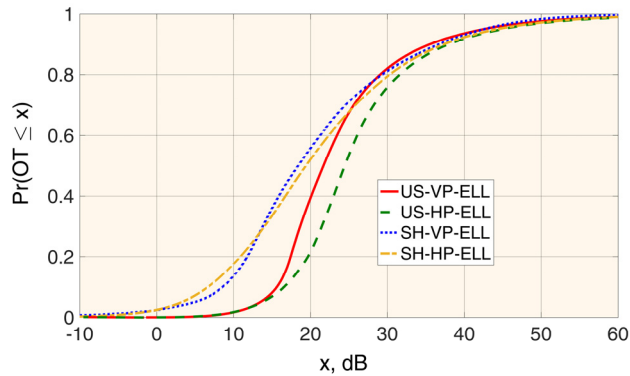


Fig. 11 – Cumulative distribution functions of OT for the ELL frequency range of the RTLs in Fig. 10 (BCI probe FCC F-130A).

c) Example of measurement results

To validate the proposed approach, an experimental campaign has been carried out with a realistic test setup mimicking a typical harness and equipment for aerospace applications. In particular, the cable harness consists of four unshielded TWPs of length 1.5 m, with terminal Sub-D connectors. Terminal units were designed and constructed using passive components (resistors, inductors, capacitors) to qualitatively reproduce the typical frequency response of the CM impedance of real-world equipment. Additionally, they were provided with interfaces to measure the RF currents induced by an RS test or injected by a BCI test. The units were in contact with the metallic floor of a semi-anechoic chamber and the cable under test was lied at constant height $h = 5$ cm above ground. The antenna elevation was set to 73° . The incident field was calibrated to 1 V/m in the frequency range 30 MHz – 1 GHz. For execution of the BCI test in the same frequency range, a BCI probe SOLAR 9129-1N was calibrated using the proposed test levels (see Fig. 10). An extensive test campaign was carried out to collect data sets for estimation of the OT cumulative distribution function. Indeed, all the obtained results corroborate the validity of the proposed approach. As a specific example, Fig. 12 shows the frequency response on the power versus frequency in the interface of a terminal unit, in case of RS testing with VP (blue line), and BCI testing (red, orange, and green lines, for three different probe positions along the cable length). It is worth noting that the low probability of undertesting ($OT \leq 0$), previously observed by the theory (see Fig. 11), is confirmed. More details

on the comparison between experimental and predicted quantiles of OT, as well as an overview and discussion of different test cases (VP/HP, unshielded/shielded) can be found in [13].

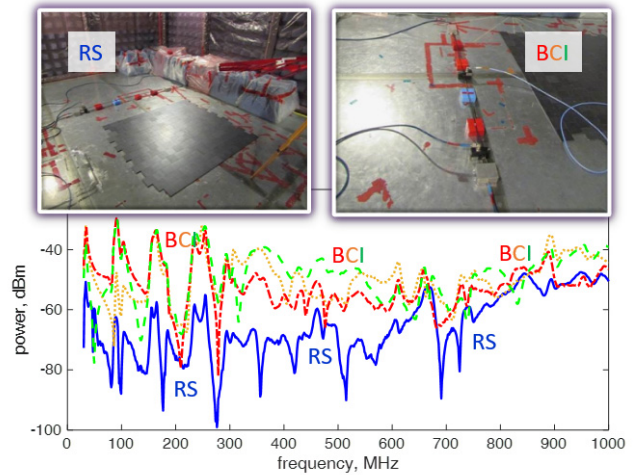


Fig. 12 – RF power measured in a specific interface of a unit in the RS test setup (HP, unshielded cable) and in the BCI test setup (test levels for HP, unshielded cable, ELL frequency range) for three different positions of the probe.

IV. Conclusion

As the electronic units on-board spacecraft operate in harsh electromagnetic environments, RS testing for the aerospace sector is of major importance and involves demanding measurement activities. Increasing physical insight in the electromagnetic coupling mechanisms, reducing EMC test complexity and relevant costs, and providing new EMC analysis tools which can be exploited at the early design stages (for pre-compliance EMC assessment) is therefore of crucial importance and worth the attention of both the scientific and the industrial EMC communities.

The alternative techniques for RS testing briefly reviewed in this article have been recently developed in the aforementioned context, with the twofold aim of improving knowledge on the involved EMC phenomena and simplifying test activity, while preserving the basic features required for implementation in real industrial settings.

In essence, if we look over the two theoretical approaches here discussed, the one based on statistical equivalence between RS an injection (making use of BCI) appears to be more promising as the use of statistics inherently allows for managing partial knowledge of the large set of parameters and data typically involved in complex setups.

Indeed, experimental results obtained by running a wide measurement campaign on several kinds of power/signal interfaces (terminal units with different CM impedances) have shown pretty good correlation between theoretical (OT cdfs) and experimental results (empirical cdfs) with a general trend towards overtesting. All the considered setups were tested for RS in an anechoic chamber and with the proposed BCI test, and the results were then compared in statistical terms.

A further outcome is that the involved test levels (for ELLs) are larger for vertical than for horizontal polarization, for setups involving both unshielded and shielded cables. This basically shows that at high frequency there is no need for running BCI tests for horizontal polarization as far as the terminal units under analysis have passed immunity verifications for vertical polarization. Among the negative aspects, it should be noted that hybrid bundles composed both of unshielded and shielded cables (often present in spacecraft) cannot at the moment be treated with the aforementioned rationale. This remains an open issue to be addressed in future investigations.

To conclude, it is worth mentioning that all the alternative tests proposed in this article do not need to be operated in an anechoic environment. The resulting advantages in terms of lower cost and quicker testing time stem basically from this consideration, and can be readily quantified once specific setups and testing procedures are selected and compared.

References

- [1] European Cooperation for Space Standardization, Space Engineering - EMC, ECSS-E-ST-20-07C, Rev. 1, 7 Feb. 2012.
- [2] Environmental Conditions and Test Procedures for Airborne Equipment, Section 20: Radio Frequency Susceptibility (Radiated and Conducted), RTCA-EUROCAE, RTCA DO-160F, Dec. 6, 2007.
- [3] Requirements for the Control of Electromagnetic Interference Characteristics of Subsystems and Equipment, Dept. Def. Interface Std., MIL-STD-461E, Aug. 20, 1999.
- [4] A. K. Agrawal, H. J. Price, and S. H. Gurbaxani, "Transient response of multiconductor transmission lines excited by a nonuniform electromagnetic field," *IEEE Trans. Electromagn. Compat.*, vol. 22, no. 2, pp. 119–129, May 1980.
- [5] F. Grassi, G. Spadacini, F. Marliani, and S. A. Pignari, "Use of double bulk current injection for susceptibility testing of avionics," *IEEE Trans. Electromagn. Compat.*, vol. 50, no. 3, pp. 524–535, Aug. 2008.
- [6] F. Grassi, F. Marliani, S. A. Pignari, "Circuit modeling of injection probes for bulk current injection," *IEEE Trans. Electromagn. Compat.*, vol. EMC-49, no. 3, pp. 563–576, Aug. 2007.
- [7] F. Grassi, H. Abdollahi, G. Spadacini, S. A. Pignari, and P. Pelissou, "Radiated immunity test involving crosstalk and enforcing equivalence with field-to-wire coupling," *IEEE Trans. Electromagn. Compat.*, vol. 58, no. 1, pp. 66–74, Feb. 2016.
- [8] C. R. Paul, *Analysis of Multiconductor Transmission Lines*, 2nd ed. New York, NY, USA: Wiley, 2008.
- [9] K. Yuan, F. Grassi, G. Spadacini, S. A. Pignari, "Reproducing field-to-wire coupling effects in twisted-wire pairs by crosstalk," *IEEE Trans. Electromagn. Compat.*, vol. 60, no. 4, Aug. 2018, pp. 991–1000.
- [10] *Road Vehicles - Component Test Methods for Electrical Disturbances from Narrowband Radiated Electromagnetic Energy: Harness Excitation Methods*, ISO 11452-4, Dec. 2011.
- [11] L. Badini, G. Spadacini, F. Grassi, S. A. Pignari and P. Pelissou, "A rationale for statistical correlation of conducted and radiated susceptibility testing in aerospace EMC," *IEEE Trans. Electromagn. Compat.*, vol. 59, no. 5, pp. 1576–1585, Oct. 2017.
- [12] G. Spadacini, L. Badini, F. Grassi, S. A. Pignari, and A. Piche, "Enforcing correlation between conducted and radiated susceptibility test setups for aerospace involving shielded cables," in *Proc. Joint IEEE EMC and Asia-Pacific Int. Symp. on Electromagn. Compat.*, Singapore, May 14–18, 2018, pp. 1–6.
- [13] G. Spadacini, F. Grassi, S. A. Pignari, P. Bisognin, and A. Piche, "Bulk current injection as an alternative radiated susceptibility test enforcing a statistically quantified overtesting margin," *IEEE Trans. Electromagn. Compat.*, vol. 60, no. 5, pp. 1270–1278, May 2018.



Sergio A. Pignari (M'01-SM'07-F'12) received the Laurea (M.S.) and Ph.D. degrees in electronic engineering from Politecnico di Torino, Turin, Italy, in 1988 and 1993, respectively.

From 1991 to 1998, he was an Assistant Professor with the Dept. of Electronics, Politecnico di Torino, Turin, Italy. In 1998, he joined Politecnico di Milano, Milan, Italy, where he is currently a Full Professor of Circuit Theory and Electromagnetic Compatibility (EMC) at the Dept. of Electronics, Information, and Bioengineering, and Chair of the B.Sc. and M.Sc. Study Programmes in Electrical Engineering, term 2015-20. He is the author or coauthor of more than 200 papers published in international journals and conference proceedings. His research interests are in the field of EMC and include field-to-wire coupling and crosstalk, conducted immunity and emissions in multi-wire structures, statistical techniques for EMC prediction, and experimental procedures and setups for EMC testing. His research activity is mainly related to Aerospace, Automotive, Energy, and Railway industry sectors. Dr. Pignari is co-recipient of the 2005 and 2016 IEEE EMC Society Transactions Prize Paper Award, and a 2011 IEEE EMC Society Technical Achievement Award. He is currently serving as an Associate Editor of the *IEEE TRANSACTIONS ON ELECTROMAGNETIC COMPATIBILITY*. From 2010 to 2015 he served as the IEEE EMC Society Chapter Coordinator. From 2007 to 2009 he was the Chair of the IEEE Italy Section EMC Society Chapter. He has been Technical Program Chair of the ESA Workshop on Aerospace EMC since 2009, and a Member of the Technical Program Committee of the Asia Pacific EMC Week since 2010. He is a member of the International Academic Committee of The State Key Laboratory of Electrical Insulation and Power Equipment (SKLEIPE) at Xi'an Jiaotong University (XJTU), Xi'an, China, term 2015-20.



Giordano Spadacini (M'07, SM'16) received the Laurea (M.Sc.) and Ph.D. degrees in Electrical Engineering from Politecnico di Milano, Milan, Italy, in 2001 and 2005, respectively, where he is currently an Associate Professor with the Department of Electronics, Information and Bioengineering. His research interests include distributed parameter circuit modeling, statistical models for the characterization of interference effects, experimental procedures and setups for EMC testing, and EMC in aerospace and railway systems.

Dr. Spadacini was awarded the 2005 IEEE EMC Transactions Prize Paper Award, the 2016 Richard B. Schulz IEEE EMC Transactions Best Paper Award, the Best Symposium Paper Awards of the 2015 Asia-Pacific Symp. on EMC (APEMC) and of the 2018 Joint IEEE EMC and APEMC Symposium.



Flavia Grassi (M'07-SM'13) received the Laurea (M.S.) and Ph.D. degrees in electrical engineering from Politecnico di Milano, Milan, Italy, in 2002 and 2006, respectively, where she is currently an Associate Professor with the Dept. of Electronics, Information and Bioengineering. From 2008 to 2009, she was with the European Space Agency (ESA), The Netherlands. Her research interests include

distributed-parameter circuit modeling, statistical techniques, measurement setups for EMC testing (aerospace and automotive sectors), and application of the powerline communications technology on ac and dc lines.

Dr. Grassi was awarded the International Union of Radio Science (URSI) Young Scientist Award at the 2008 URSI General Assembly, and the IEEE Young Scientist Award at the 2016 Asia-Pacific Int. Symp. on EMC (APEMC). She was a recipient of the 2016 Richard B. Schulz IEEE EMC Transactions Best Paper Award, of the Best Symposium Paper Awards of the 2015 APEMC Symposium and of the 2018 Joint IEEE EMC and APEMC Symposium.